

Emulsion and Miniemulsion Polymerization of Isobornyl Acrylate

Alan J. Back, F. Joseph Schork

School of Chemical and Biomolecular Engineering, Georgia Institute of Technology, Atlanta, Georgia 30332-0100

Received 26 April 2006; accepted 2 July 2006

DOI 10.1002/app.25181

Published online in Wiley InterScience (www.interscience.wiley.com).

ABSTRACT: Isobornyl acrylate, a highly hydrophobic monomer, was batch-polymerized in both emulsion and miniemulsion recipes. Surfactant levels above and below the critical micelle concentration were used, as were two different initiator types: ionic (potassium persulfate) and nonionic (*t*-butyl hydroperoxide). Samples were analyzed for degree of conversion, molecular weight, and particle size. The effects of reaction type (emulsion versus miniemulsion), surfactant

level, type of initiator (ionic versus nonionic) of the polymer properties are discussed. Issues of monomer transport across the aqueous phase, and mechanisms of nucleation, especially at very low surfactant concentrations are discussed. © 2006 Wiley Periodicals, Inc. *J Appl Polym Sci* 103: 819–833, 2007

Key words: polymerization; emulsion; isobornylacrylate; miniemulsion

INTRODUCTION

In the field of dispersed-phase polymerization, certain reaction routes and starting materials are frequently associated with one another. Monomers that display some degree of water solubility, such as styrene and vinyl acetate, are regarded as good candidates for emulsion polymerization. Water-soluble initiators are most often used with systems of this type. When the monomer is very much less miscible with water, suspension polymerization is the alternative most often employed; species such as long-chain acrylates fall into this category. In these cases, initiators that readily dissolve in the organic phase (the “oil”) usually come into play.

While such generalizations are useful for academic purposes, they fail to take into account the many factors that can affect the dominant polymerization route in a given system. Replacing an ionic (water-soluble) initiator with a nonionic, oil-soluble one encourages bulk polymerization kinetics even when the monomer can diffuse through the aqueous phase, for example. Conversely, if a hydrophobic monomer can be made to diffuse quickly enough to feed a growing chain, the end result will be a proliferation of emulsion polymer particles. Needless to say, the possible combinations of additives and recipe modifications vary greatly, as do the effects they can have on a particular system.

A consideration of the details of each type of reaction is in order. In suspension polymerization, the

monomer droplets are typically very large, on the order of hundreds of microns, and may have a layer of stabilizer molecules at their surface. This is a compound, usually water-soluble, that helps to retard coagulation of the particles during reaction. They may work by increasing the aqueous-phase viscosity, creating steric hindrance to coagulation, providing electrostatic repulsion between particles (if the stabilizer is ionic), or some combination of these methods.

Particles from a suspension polymerization are generally in the 10–1000 μm range, while those produced in an emulsion are usually smaller than 1 μm due to the different steps involved in starting the reaction. Also, initiation and termination steps take place in different phases for each scenario. For suspension polymerization, chains are both initiated and terminated in the organic phase, while in an emulsion the initiation step occurs in the aqueous phase. Termination occurs when a new radical is captured by a particle that already contains a growing chain; the small volume to which they are confined forces them together and stops them from reacting further.

Monomers that have a high degree of water solubility, such as acrylamide, can undergo homogeneous nucleation under certain circumstances. Aqueous-phase radicals can propagate to such a degree that they are able to coagulate with one another and form a precursor particle; this is then fed by diffusion as previously described. This mechanism has been proposed to explain the phenomenon of surfactant-free emulsion systems.

While radicals are more likely to be captured by micelles than droplets in an emulsion, the latter pathway is not a complete impossibility and must be

Correspondence to: F. J. Schork (joseph.schork@chbe.gatech.edu).

taken into account if the droplet size is not vastly greater than that of the micelles/small particles. The extreme case comes when micelles are eliminated, which can happen if the surfactant level is very low or the droplets are made very small as in a miniemulsion. This last type of reaction generally requires the addition of an extremely hydrophobic component, often referred to in error as a "cosurfactant" (more recently, "costabilizer"), to hinder diffusion of monomer out of the droplets.

Conventional wisdom holds that emulsion polymerization requires a monomer with some water solubility, a hydrophilic initiator, and a surfactant concentration higher than the critical micelle concentration (CMC). The CMC is the point at which micelles begin to form.

The goal of this work is to investigate the mass transfer and radical flux phenomena at work in dispersed-phase polymerization of isobornyl acrylate (IBoA), using different water-soluble initiators in both emulsion and miniemulsion formulations. This monomer was used because it displays a high degree of hydrophobicity and forms a polymer with a high glass transition temperature ($\sim 90^\circ\text{C}$).¹ An examination of the processes at work on the molecular level will provide new insight into the behavior and modeling of dispersed-phase reactions.

THEORY

Emulsion polymerization

In the classical theory proposed by Rodriguez,² an emulsion polymerization can be divided into three intervals. At the beginning, monomer is present as large droplets that are partially or totally covered with a layer of surfactant molecules. Additional surfactant is present in the aqueous phase as either free molecules or micelles; these latter are only present if the critical micelle concentration (CMC) has been exceeded. During Interval I, micelles swollen with monomer capture initiator radicals that have propagated to a critical chain length in the aqueous phase. These newly nucleated particles grow by diffusion of monomer from the droplets and must adsorb more surfactant to stabilize the additional surface area thus formed. Interval II starts when the micelles have been consumed, either by being nucleated to form particles, or by disappearing to supply surfactant to the growing interfacial area of the existing particles. This point marks the end of primary nucleation. A roughly constant polymerization rate is established as monomer continues to diffuse from the droplets and across the aqueous phase. The rate R_p is given by²

$$R_p = \frac{k_p[M]_p\bar{n}N_p}{N_A} \quad (1)$$

where N_p is the particle number, $[M]_p$ is the monomer concentration within the particles, and k_p is the propagation rate constant, N_A is Avogadro's number, and \bar{n} is the average number of radicals per particle. Deviations from this model are not uncommon. Ghielmi and coworkers state that if \bar{n} is very small (say, 0.01), the probability of a new radical entering a particle that already has one is very small. Hence, termination by coupling can be ignored and the system can be modeled as a bulk polymerization in which the radical concentration is equal to that in the particles. According to the authors, the frequency of radical exit from the particles must be high and the initiation rate low to achieve this situation.³ At the other extreme is the pseudobulk system, in which \bar{n} is considerably higher than 0.5.

Miniemulsion polymerization

In a miniemulsion system, a hydrophobic additive is typically added to the monomer. This may be a long-chain hydrocarbon such as hexadecane, a long-chain alcohol such as cetyl alcohol, or even a polymer. These materials are often referred to as "cosurfactants," a term that is slightly in error here as they generally do not alter the surface activity of the droplets or particles. (A more recent and more accurate term is "costabilizer.") The additive's primary function is to hinder diffusion of the monomer into the aqueous phase, where it can swell surfactant micelles. Radicals therefore tend to be selectively captured by the droplets, which act as tiny bulk reactors. Equation (2) is not applicable for miniemulsions, but only if one realizes that the monomer concentration within particles will not be constant; there is no outside source to keep feeding them. The system starts to resemble Interval III of Smith-Ewart kinetics once the particles are nucleated.

EXPERIMENTAL

Estimation of properties: mass transfer and kinetics

Monomer diffusivities at the reaction temperatures were estimated using the Wilke-Chang correlation given by Skelland⁴ and densities and viscosities from the literature. The results are summarized in Table I; in each case, the specific volume of the diffusing species was taken as that of the pure component.

TABLE I
Estimated Molecular Diffusivities of Monomer Radicals

Species A	Phase B	T ($^\circ\text{C}$)	M_A	D_{AB} (cm^2/s) ^a
IBoA	H ₂ O	50	208.30	1.20×10^{-5}
IBoA	H ₂ O	30	208.30	7.72×10^{-6}

^a Estimated by Wilke-Chang correlation given in Ref. 5.

TABLE II
Recipes for Emulsion Polymerization
of IBoA, using KPS

Run no.	H ₂ O (g)	IBoA (g)	KPS (mmol/L)	SLS (mmol/L)
A	271.77	94.65	10.036	0.000
B	271.67	94.97	10.053	0.999
C	272.30	94.67	10.011	1.996
1	272.03	95.00	10.010	2.996
2	272.42	94.99	9.995	4.002
3	272.01	94.55	10.004	5.992
4	272.81	94.80	9.988	7.967
5	272.31	94.95	9.997	9.986
6	272.05	95.59	9.986	12.507
7	272.03	95.02	10.004	14.997
8	272.18	94.76	10.002	19.975

All reactions carried out at 50°C and 300 rpm stirring.

Reagent preparation

IBoA (Aldrich) was first treated to remove the hydroquinone monomethyl ether that had been added by the manufacturer to inhibit polymerization. An aqueous wash solution of 10 wt % sodium hydroxide, saturated with sodium chloride, was mixed with the monomer and subjected to magnetic stirring for 30 min. The volume ratio of monomer to solution was ~ 5 : 1. The mixture was then poured into a separatory funnel and left standing overnight to allow the phases to split; the aqueous phase was discarded and the monomer treated with a few grams of calcium sulfate to remove any residual water. Finally, the solids were removed by vacuum filtration.

Redox components—*t*-butyl hydroperoxide (*t*-BHP; Aldrich), sodium formaldehyde sulfoxylate (SFS; Fluka), ferrous sulfate, and disodium ethylenediamine tetraacetate (NaEDTA; both Fisher)—were made into stock solutions at 100 times the concentration required for those particular reactions. Hexadecane (HD), sodium lauryl sulfate (SLS), and potassium persulfate (KPS) (all from Aldrich) were used as delivered.

TABLE III
Recipes for Emulsion Polymerization
of IBoA, using *t*-BHP

Run no.	H ₂ O (g)	IBoA (g)	<i>t</i> -BHP (mmol/L)	SLS (mmol/L)
1	272.50	95.27	1.008	3.001
2	273.00	95.42	0.997	3.982
3	272.84	95.11	0.997	5.980
4	273.34	95.00	0.996	7.957
5	272.88	95.24	0.999	9.968
6	272.29	94.49	1.000	12.470
7	273.28	95.01	0.995	14.925
8	273.02	95.02	0.997	19.922
9	272.93	94.99	1.001	24.918
10	273.12	94.99	0.993	29.828

All reactions carried out at 30°C and 300 rpm stirring.

TABLE IV
Recipes for Miniemulsion Polymerization
of IBoA, using KPS

Run no.	H ₂ O (g)	IBoA (g)	KPS (mmol/L)	SLS (mmol/L)	HD (g)
1	272.42	94.84	9.993	4.981	1.90
2	272.33	94.45	10.003	8.002	1.91
3	272.51	94.97	9.972	9.972	1.92
4	272.17	95.17	9.988	12.473	1.92
5	272.48	94.68	9.986	14.966	1.94
6	272.27	94.74	9.991	17.468	1.96
7	272.30	95.67	9.992	19.958	1.93
8	272.16	94.66	10.001	24.986	1.93
9	272.75	95.32	9.977	29.906	1.92

All reactions carried out at 50°C and 300 rpm stirring.

Tables II–V give the details of all recipes used in this work.

Reaction apparatus

For all experiments, a 500-mL batch reactor, fitted with stirring motor and water-cooled condenser, was used. The vessel was heated by a thermostat-controlled water bath and could be purged with nitrogen as needed.

Emulsion polymerization (KPS initiator)

To prepare the equipment, the reactor was assembled and the water bath heater was started with a setpoint of 50°C. The nitrogen purge was started at high speed (~ 3–4 mL/s) to allow ample time for the oxygen to be flushed out; at the same time, the stirrer was activated at a speed of 300 rpm and the condenser cooling water was started.

The required quantity of water was weighed out and a small quantity set aside for later use with the KPS. Next, the required amount of SLS was added to the bulk of the water and allowed to dissolve. The monomer charge was then added to the solution and stirred magnetically for 30 min. By the end of this

TABLE V
Recipes for Miniemulsion Polymerization
of IBoA, using *t*-BHP

Run no.	H ₂ O (g)	IBoA (g)	<i>t</i> -BHP (mmol/L)	SLS (mmol/L)	HD (g)
1	272.88	95.34	1.001	2.986	1.94
2	273.07	95.14	1.000	4.974	1.92
3	272.07	95.53	1.005	7.005	1.90
4	273.01	95.46	0.999	9.938	1.93
5	272.68	95.28	1.001	12.929	1.95
6	272.89	94.94	0.999	14.922	1.94
7	272.11	94.47	1.000	19.990	1.92
8	272.75	95.60	1.000	24.862	1.90

All reactions carried out at 30°C and 400 rpm stirring.

time, the reactor had been purging for at least 60 min and the water bath was up to the desired temperature. The batch was then loaded in and put under fast purge for 2–3 min to remove any oxygen that had entered in this step. Next, the nitrogen was slowed and the reactor left to equilibrate for 30 min.

Near the end of this time, the required KPS was dissolved in the water that had been set aside. This solution was injected into the reactor to mark the start of the polymerization. For the next 120 min, samples were withdrawn at 10-min intervals and mixed with preweighed amounts of cold hydroquinone solution (0.5 wt % in water) to short-stop the reaction.

Emulsion polymerization (*t*-BHP initiator)

For the reactions employing *t*-BHP, the procedure was much the same as that just described, with the following changes. First, the reactor was heated to 30°C. Second, the amount of water measured out was lowered to account for that which would be introduced with the redox component stock solutions. Third, a few grams of water were still set aside, but for mixing with the stocks. Fourth, to start the reaction, these reagents were injected at 10-min intervals: SFS, *t*-BHP, FeSO₄ (complexed with NaEDTA in a 2.1 : 1 EDTA/Fe²⁺ mole ratio). This procedure was based on that used by Hamersveld⁶ in his study of oil/acrylic hybrid latex systems.

Miniemulsion polymerization

The miniemulsion experiments were set up according to the same procedure as their emulsion counterparts, with the following changes. Before stirring began, HD was added to the monomer phase to give a 50 : 1 weight ratio of the latter to the former. Stirring lasted for 60 min, after which the batch was sonicated with a Fisher Model 300 Sonic Dismembrator, set to 70% relative output, for 20 min. This equipment generated a significant amount of heat in the mixture, but preliminary tests revealed that the temperature rise did not cause polymerization to start in the absence of initiator. Therefore, no cooling bath was used during the sonication; however, the container was covered to minimize liquid loss from evaporation.

Routine sample analysis

To determine the degree of conversion gravimetrically, small amounts of the samples were measured into preweighed pans and dried in an oven overnight at 70–90°C. The resulting solids content was corrected for nonvolatile salts and additives to find the actual polymer formed. Although IBoA has a very high boiling point (~ 115°C at 15 mmHg), the

drying temperatures were found to be sufficient to drive off the unreacted material after one night. This observation was confirmed by subjecting a small quantity of the washed monomer to the same conditions. The next morning, the liquid had completely evaporated and there was no solid residue, indicating that thermal generation of free radicals was not taking place to cause polymer to form in the oven.

Molecular weights were determined by gel permeation chromatography (GPC) using two columns. The first (Phenomenex) had a pore size of 10³ Å, while the second (Viscotek) was a mixed-bed column designed to give a linear calibration. However, it was found that putting the small-pore column in front gave better accuracy with known standards. A Waters 410 differential refractometer and Viscotek T60A detector provided data to the TriSEC 3.0 software (Viscotek). Tetrahydrofuran (THF) was used both as eluent and as solvent for the samples; solutions were made up to overall concentrations of 3–8 mg polymer/mL liquid. These were then filtered to remove any insoluble material and then injected into the system, passing through a second filter before entering the columns and detector. Poly(methyl methacrylate) standards were used for the calibration, with the molecular weights of these being corrected for the polymers formed in this work. Assuming that the columns perform their separation based on hydrodynamic volume $M[\eta]$ of the polymer molecules, the adjustment is fairly straightforward. The Mark-Houwink-Sakurada equation predicts:

$$[\eta] = KM^a \quad (2)$$

where K and a are parameters that have been tabulated for many polymers. If molecules of equal hydrodynamic volume have the same elution time, then for an unknown and a reference, the following holds:

$$K_{\text{ref}}M_{\text{ref}}^{a,\text{ref}+1} = KM^{a+1} \quad (3)$$

Rearranging,

$$M = \left[\frac{K_{\text{ref}}}{K} \right]^{\frac{1}{a+1}} (M_{\text{ref}})^{\frac{a,\text{ref}+1}{a+1}} \quad (4)$$

Since exact parameters for poly(IBoA) are hard to come by, it is necessary to estimate them based on values for structurally similar materials. Linear regression on MHS parameters for various methacrylate polymers in THF and correcting the proportionality constant for the lack of the extra methyl group in the actual polymer yields the following correlation between the standards and poly(IBoA):

$$M = 1.141(M_{\text{ref}})^{0.994} \quad (5)$$

Equation (13) is only strictly valid for linear polymer; varying levels of branching may introduce some error, but this is not thought to be highly significant.

Particle size distributions were obtained by dynamic light scattering, using a Protein Solutions DynaPro system connected to the company's Model LSR micro-sampler. A drop of sample was placed in a cuvette and diluted with deionized water, to a volume of roughly 4 mL, or a 100 : 1 volume ratio. This mixture was then diluted further until it gave a count rate that did not exceed the detector's upper limit; in most cases, this entailed another 100 : 1 addition of water. Twenty measurements were taken per sample.

Additional analyses

Polymer density was determined by dissolving a few grams of a final latex batch in THF and allowing the solution to dry overnight. A small amount of the dried material was then placed in a measured amount of water, and glycerin was added until the sample began to float. Viscosities of the organic and aqueous phases at the temperatures of interest were measured with a Brookfield RVTDV-1 Digital Viscometer. Monomer density was listed by the manufacturer as 0.986 g/cm^3 (25°C).

The CMC of the surfactant under various reaction conditions was found through molar conductivity measurements. A solution with the appropriate additives (*t*-BHP or KPS, according to the recipe) was made up and half of it set aside, while sufficient SLS was dissolved in the other half to raise it well above the CMC and this mixture was heated to the desired temperature. The solution without surfactant was added a little at a time, and the conductivity was measured after each step. To determine the CMC, molar conductivity (meter reading divided by SLS concentration) was plotted and fitted to a piecewise linear model to pinpoint the discontinuity in the values, using the squared residuals as the criterion.

The solubility of IBoA was measured by adding a known quantity of the monomer to 1 L water, stirring the mixture thoroughly, and allowing the phases to separate overnight. Based on the thickness of the organic layer floating on top and the geometry of the flask, the amount of dissolved material could be calculated.

RESULTS AND DISCUSSION

The polymer density was determined as 1.021 g/cm^3 , based on the mass fraction of glycerin needed to make the solid sample begin to float (10.0% in water) and using solution properties given by Perry.⁷ Solubility of IBoA was determined to be 85 ppm by weight (0.41 mM). This figure is comparable with the result reported by Vanderhoff for isooctyl acrylate (62 ppm).⁸ The method described earlier is admittedly prone to errors. Chai et al.⁹ have used a much more precise

method, and report the solubility of IBoA as 3 ppm, and that of isooctyl acrylate as 29 ppm. (All monomer solubilities are quoted at 25°C .) The question of whether species as hydrophobic as this can reasonably be expected to follow Smith-Ewart kinetics will be addressed shortly.

Polymerization kinetics

Figure 1 shows the conversion time curves for emulsion polymerization with KPS as initiator. There are a number of features worth noting. First, it is possible to do surfactant-free emulsion polymerization with this system (Run A), although the rates are low. This is not unexpected. Surfactant-free polymerization is known. The persulfate end groups form an *in situ* surfactant. Second, polymerization at high rates is possible below the CMC. The CMC for this system was measured as 7.8 mM. Runs A–C and 1–4 are substantially below the CMC. Polymerization is likely possible because of the additional stabilization provided by the KPS end groups. Third, as the surfactant level is increased the rate of polymerization increase, due to the increase in

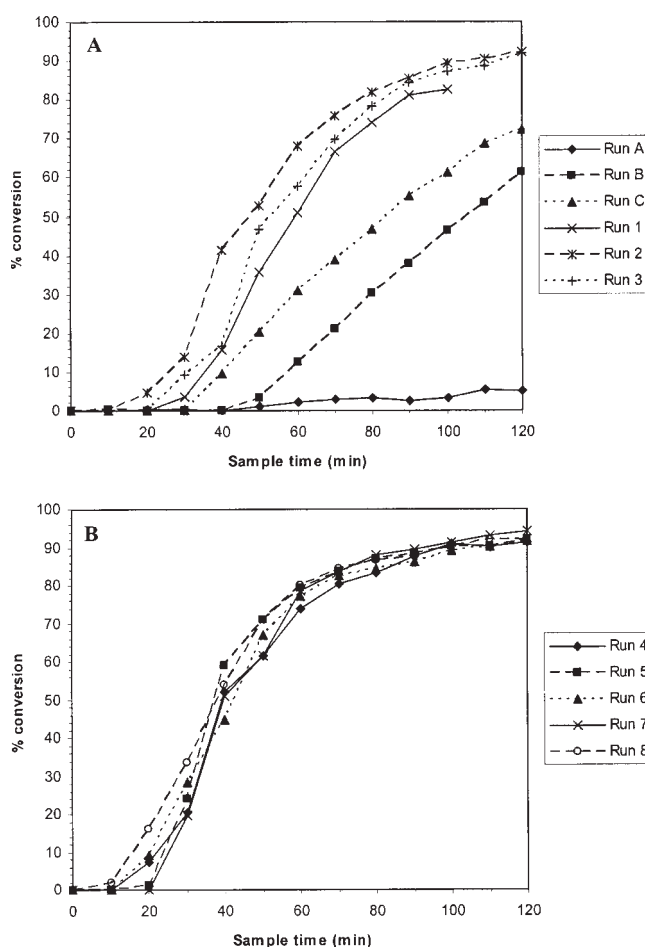


Figure 1 Conversion profiles: IBoA emulsions with KPS. A. Low SLS concentrations; B. High SLS concentrations.

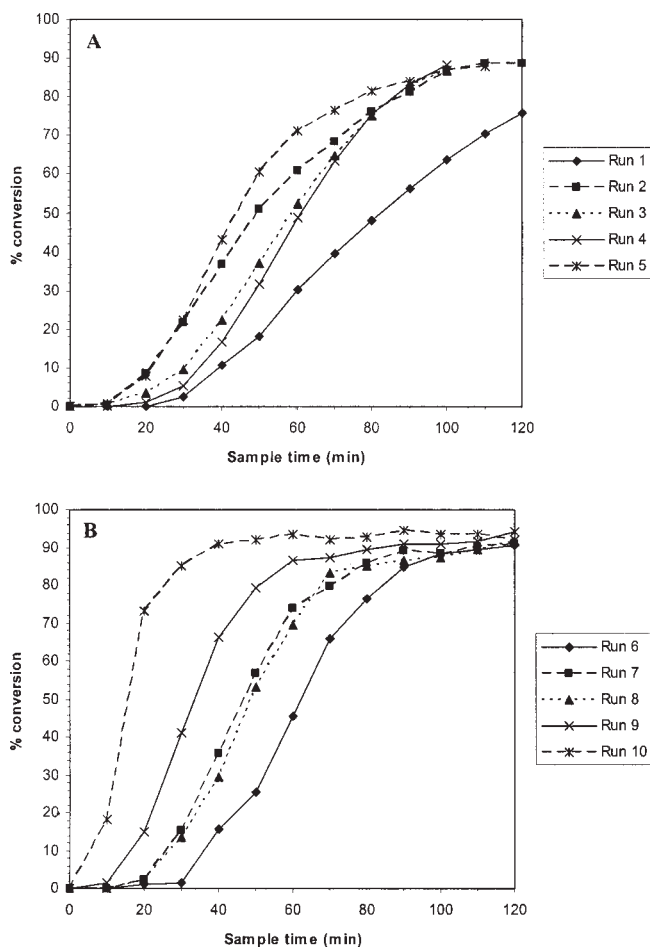


Figure 2 Conversion profiles: IBoA emulsions with *t*-BHP. A. Low SLS concentrations; B. High SLS concentrations.

the number of polymer particles as will be seen later in Figure 5. Fourth, there are significant lag times before polymerization begins. This is attributable to low levels of inhibitor, which can have an abnormally high impact in highly water-insoluble monomer as described by Schork and Back¹⁰ or, to the very slow rate of growth of oligomers in the aqueous phase due to the low water solubility of the monomer (causing very slow growth of water-phase oligomers, and slow particle nucleation). Finally, at high surfactant concentrations, there is little effect of surfactant level on rate of polymerization. This is due to the high level of surfactant, plus the stabilizing effect of the KPS end groups. Micellar nucleation is likely limited by radical flux rather than by surfactant concentration.

Figure 2 shows the conversion time curves for emulsion polymerization with *t*-BHP as initiator. This initiator resides primarily in the aqueous phase. Since the reductant of the redox pair (FeSO_4) is water-soluble, the preponderance of radicals will be generated in the aqueous phase. However, unlike KPS, *t*-BHP does not result in an ionic end group on the radical oligomers in the aqueous phase. This means they will have very

little surface activity. The most intriguing feature of these graphs is that polymerization at substantial rates takes place well below the CMC. Runs 1–3 are below the CMC (measured as 8.0 mM of this system). The lowest surfactant run, Run 1 is at less than 40% of the CMC, suggesting that micelles are not present. Hypotheses for nucleation in this system are given in the next section. As with KPS, there are significant lag times before polymerization begins. The same mechanisms for slow nucleation are active here as discussed earlier for the KPS runs. Finally, the high surfactant runs are much more sensitive to surfactant concentration than was the case with KPS. This is likely due to the absence of ionic end groups to act as additional *in situ* surfactant.

Figure 3 shows the conversion time curves for miniemulsion polymerization with KPS. Here we see the same lag in nucleation. The slow nucleation characteristic of highly water-insoluble monomers with a water-soluble initiator are present regardless of whether the nucleation is from micelles or droplets, since the delay is in generating oligomers in the aqueous phase. Here, the conversion time curves are

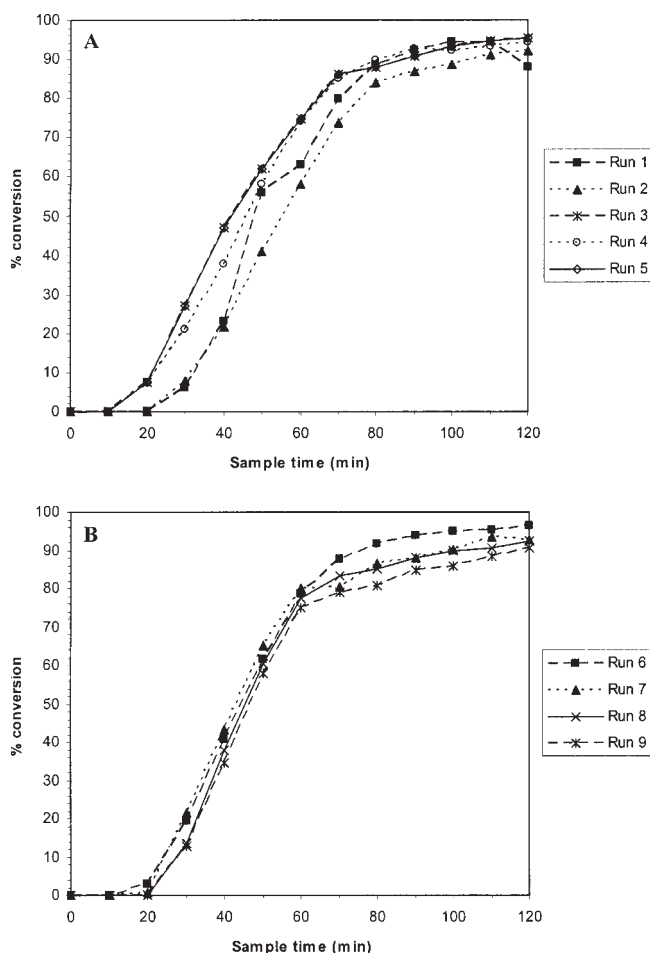


Figure 3 Conversion profiles: IBoA miniemulsions with KPS. A. Low SLS concentrations; B. High SLS concentrations.

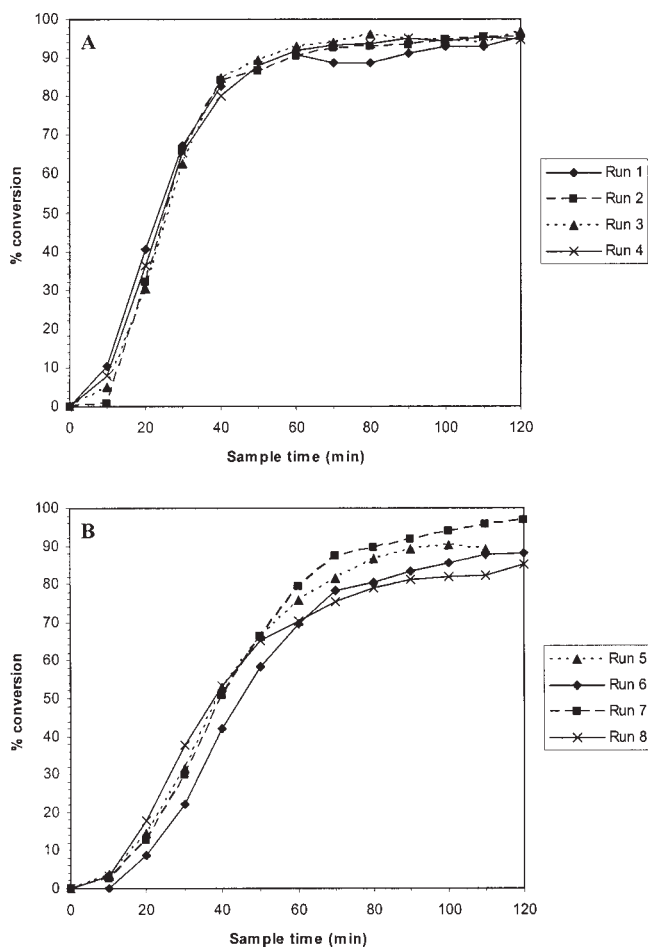


Figure 4 Conversion profiles: IBoA miniemulsions with *t*-BHP. A. Low SLS concentrations; B. High SLS concentrations.

not particularly sensitive to surfactant level, both below and above the CMC (CMC = 8.0 mM). This is due to the very different mechanism of nucleation in miniemulsions. In droplet nucleation, the rate of nucleation depends on the concentration of droplets, which is, in turn, a weaker function of surfactant concentration than the concentration of micelles in an emulsion system.

Figure 4 shows the conversion time curves for miniemulsion polymerization with *t*-BHP. Here we see much less lag in nucleation, although the reason for this is not clear. We also see a lack of sensitivity to surfactant levels, especially at higher surfactant levels, that is characteristic of miniemulsion systems.

Particle numbers

Final particle concentrations (number per unit volume of water) were calculated based on the properties of the last sample for a run, using this relation:

$$N_{cf} = \frac{x_f m_M}{\frac{4}{3} \pi (\bar{r})^3 V_W d_p} \quad (6)$$

The formula calculates the total volume of polymer (mass converted over density) and the volume of a single particle. Based on the small volume of actual latex and high dilution ratio used for the size measurement, essentially all the unreacted monomer was stripped out of the particles. The values in measured are therefore the unswollen radii.

Log-log plots of N_c versus [SLS] in the macro- and miniemulsions are shown in Figures 5 and 6, as a means of fitting the data to the Smith-Ewart correlations. It is apparent from these graphs that there is a marked discontinuity in each set, which can be compared to the CMC. Piecewise linear regression on the data points, with the break point chosen to minimize the total residuals, yields the results in the previously mentioned figures and Table VI.

It can be seen from these results that the break in the particle numbers generally corresponds well with the CMC as determined from conductivity measurements (Table VI). What this suggests is that the amount of surfactant covering the particles and droplets at low conversion is small relative to the total present in the aqueous phase. It is therefore not necessary to correct the surfactant concentration for this effect.

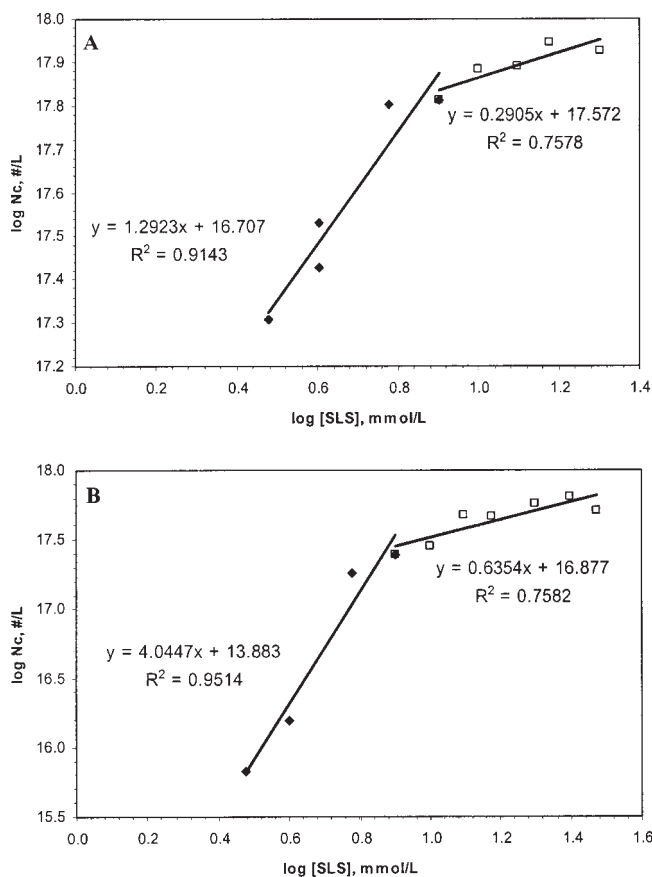


Figure 5 Particle number data for IBoA emulsions. A. 10 mM KPS; B. 1 mM *t*-BHP.

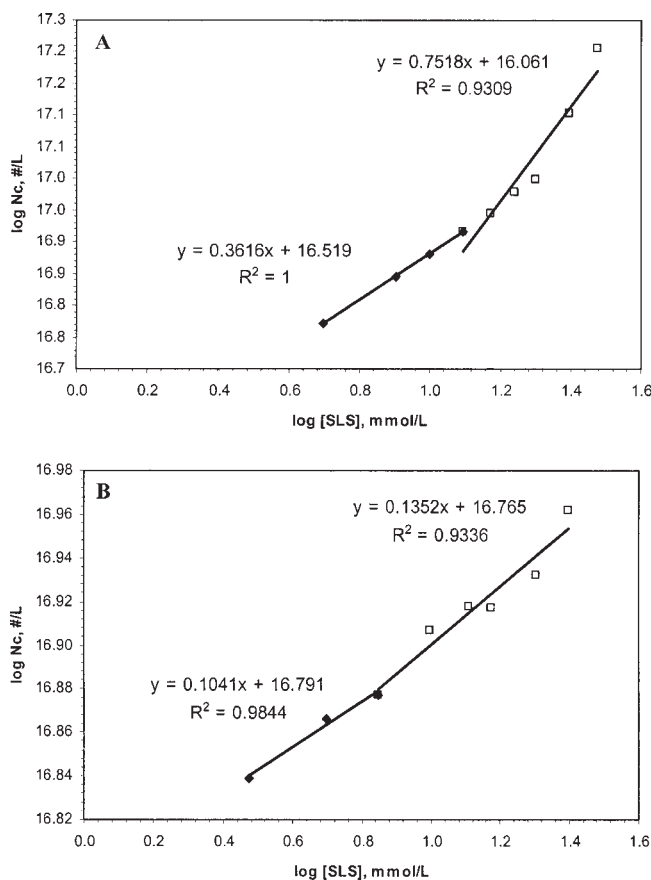


Figure 6 Particle number data for IBoA miniemulsions. A. 10 mM KPS; B. 1 mM *t*-BHP.

One trend that immediately becomes apparent is the behavior of the emulsion particle numbers as opposed to those of the miniemulsions. The emulsion particle number trends show a drop in slope after the CMC, while the miniemulsion fit shows an increase in slope. This can be explained in light of data on the particle number as a function of surfactant level, as reported by Vanderhoff⁵ in his survey of emulsion polymerization. Such a curve typically describes a sigmoid, with the point of inflection near the CMC. Nucleation at low surfactant concentration was ascribed to homogenous nucleation. Near the CMC, the rapid rise in number of particles was ascribed to micellar nucleation. The low rate of increase in particle number with surfactant concentration was ascribed to radical flux insufficient to nucleate a larger fraction of the micelles. Here, the emulsions exhibit behavior consistent with the upper portion of the curve: a sharp rise near the CMC, then a leveling off. On the other hand, the miniemulsions match the lower portion: more level particle numbers at low surfactant concentrations, then a rise past the break point. The miniemulsions exhibit behavior similar to the low surfactant end of the sigmoid, but the mechanism is very different. Here, the lower slope line corresponds to droplet nucleation rather than to homogenous nucleation which is not likely to be signifi-

cant for a monomer of such low water solubility. The steeper slope of the high surfactant line is likely due to micellar nucleation.

Monomer diffusion considerations in emulsion polymerization of IBoA

In the Smith-Ewart description of emulsion polymerization, Interval II relies on the diffusion of monomer to the growing particles from the large droplets. Emulsion polymerization is commonly assumed to be reaction, rather than diffusion limited, but with highly water-insoluble monomer (e.g., IBoA), this assumption is worth investigating. Inspection of Figures 1 and 2 shows a representative steady-state conversion rate during Interval II of 3% per minute. With a monomer charge of 95 g, this is equal to roughly 0.045 g/s, which is the minimum quantity that would have to be provided by the large droplets in order for the Smith-Ewart theory to be viable.

The starting point for evaluating the situation is to estimate the size of the droplets. During the emulsion experiments, the earliest samples that showed essentially no conversion would separate into two phases within 10 min. The height of the aqueous phase was roughly 3 cm, giving a terminal droplet velocity of 0.005 cm/s. From Stokes' law, this terminal velocity is given for low-Reynolds-number flow as follows:

$$V_{\text{sett}} = \frac{2r^2g\Delta\rho}{9\mu} \quad (7)$$

where r is the droplet radius, $\Delta\rho$ is the density difference between the droplet and the continuous phase, μ is the continuous phase viscosity, and g is the acceleration due to gravity. Rearranging the expression and inserting the appropriate physical properties for the water and monomer phases at 50°C results in a droplet radius of 60 μm for the KPS system and 70 μm for the *t*-BHP system (Table VII).

The mass transfer coefficient for monomer leaving the monomer droplets in a similar system has been estimated by Reimers¹¹ as

$$k_c = \frac{2D_w}{r} \quad (8)$$

TABLE VI
SLS Concentrations Corresponding to Transition Points in Particle Number Fits

Reaction type	[SLS] at transition (mmol/L)	CMC (mmol/L)
IBoA emul (KPS)	7.3	7.8
IBoA emul (<i>t</i> -BHP)	7.6	8.0
IBoA ME (KPS)	16.0	7.8
IBoA ME (<i>t</i> -BHP)	6.9	8.0

TABLE VII
Droplet Radii for Emulsion Recipes

Recipe	T (°C)	Water μ (cP)	Term. vel. (cm/s)	Droplet rad. (μm)
IBoA emul (KPS)	50	0.55	0.005	60
IBoA emul (<i>t</i> -BHP)	30	0.80	0.005	70

This correlation holds when the droplets are small enough that there is no surface scrubbing, an assumption that is justified for 60 μm droplets (KPS system). Estimating the diffusivity of IBoA in water at 50°C (D_w) by the Wilke-Chang correlation as $1.2 \times 10^{-5} \text{ cm}^2/\text{s}$, the value of k_c can then be estimated as $4 \times 10^{-5} \text{ m/s}$. The maximum mass transfer from the droplets, Q_M , will be given by:

$$Q_M = k_c A_{\text{drop}} ([M]_{\text{aq,sat}} - [M]_{\text{aq,bulk}}) \quad (9)$$

where A_{drop} is the total surface area of the droplets per unit volume of aqueous phase. $[M]_{\text{aq,sat}}$ is the saturation value of IBOA in water, and $[M]_{\text{aq,bulk}}$ is the concentration of IBoA in the aqueous phase far from the droplet surface. The needed Q_M to support a conversion rate of 3% per minute is $7.9 \times 10^{-4} \text{ mol/L s}$ (based on aqueous phase). Using the value of k_c above, the concentration driving force necessary to provide Q_M in the earlier expression is found to be $4.5 \times 10^{-4} \text{ mol/L}$. The value of the solubility of IBoA in water at 25°C is reported⁹ to be $1.6 \times 10^{-5} \text{ mol/L}$. Allowing for increased solubility with increased temperature, the solubility at the reaction temperature may be estimated to be of the order of magnitude of 1×10^{-4} . Thus, even if $[M]_{\text{aq,bulk}}$ were zero, it is questionable if it is possible to provide the necessary driving force do to the limitation of the value of $[M]_{\text{aq,sat}}$. All of the above-mentioned calculations are only order-of-magnitude estimates, but as such, point to the possibility that this system maybe at least partially diffusion, rather than reaction limited. If that is the case, then Smith Ewart kinetics may not be strictly applicable. It should be noted that similar considerations do not come into play in the miniemulsion polymerizations, since monomer transport in miniemulsions is not critical to the polymerization mechanism.

Particle formation in low surfactant, hydrophobic monomer systems

It will be noticed that, even at very low surfactant levels (approximately one-third of the CMC), and with a nonionic initiator (*t*-BHP), heterogeneous polymerization takes place in the IBoA emulsions. This is interesting since the droplet size was estimated at 70 μm , and therefore droplet nucleation is unlikely, and would not result in submicron particles. Likewise, micellar nucleation is very unlikely at such

low surfactant concentrations. Finally, homogenous nucleation is only considered significant with monomers of high water solubility such as vinyl acetate. Clearly, the mode of particle nucleation for these systems is not understood. During the polymerization of the emulsion recipes, it was observed that samples would separate into aqueous and large-droplet phases until some point during the quasilinear portion of the conversion profile. The aqueous phase contained the formed polymer; while the organic phase became less and less prominent until the two merged into a homogeneous mixture. Mini-emulsions exhibited a similar behavior, but on a much longer time scale due to the smaller droplet size ($\sim 100 \text{ nm}$ vs. 60–70 μm); in this case, the aqueous phase was seen to be essentially free of polymer.

In the aqueous phase, new initiator radicals propagate until they reach a certain critical chain length and become too hydrophobic to remain in solution. These can then either terminate with one another or be captured by small droplets or micelles. If termination occurs, a new oligomer is formed: one that has an initiator fragment on at least one end contains several monomer units. If the initiator fragment is hydrophilic, this species can act as a combination surfactant and/or hydrophobe. In the KPS systems, the charged initiator fragment will cause the oligomers to be surface active. In fact, surfactant-free emulsion polymerization with KPS is well known, and is demonstrated in Figure 1. When an uncharged initiator (e.g., *t*-BHP) is used, there is little basis for oligomers-as-surfactant.

Wang and Poehlein investigated the issue of critical chain length (for capture or association with other aqueous species) in their work with emulsion copolymerization of styrene with more hydrophilic comonomers. When acrylic acid was used, critical lengths of 8–11 units were found, decreasing to 5–6 and 3–4 after methacrylic acid and methyl methacrylate were employed instead, respectively.¹² This marked decrease in length supports the idea that more hydrophobic monomers become capable of being captured after fewer aqueous propagation steps. The fact that IBoA is roughly an order of magnitude less soluble than styrene suggests an even shorter critical chain length at work in the systems studied here.

One hypothesis for the nucleation of submicron particles is a sort of homogenous nucleation in which oligomers combine with surfactant dissolved in the aqueous phase. These precursor particles then combine to form polymer particles. An alternate view is that active oligomeric radicals do not accumulate in the aqueous phase until the collection becomes large enough to precipitate. Instead, live and dead oligomers combine with surfactant molecules and adsorb onto the surface of particles. Under the force of agitation, small droplets will be broken off of the large

TABLE VIII
Experimental Data: Molecular Weights and Particle Size

Recipe type	Run no.	Sample time (min)	M_n (10^{-3} g/mol)	M_w (10^{-3} g/mol)	Unsw. part. radius (nm)
IBoA Emul (KPS)	1	70	1,828	4,596	49.37
		80	1,543	4,167	56.53
		90	1,135	3,757	62.62
		100	1,287	3,840	66.57
		110	1,169	3,716	66.04
		120	1,097	3,402	67.21
	2	50	1,625	4,126	49.05
		60	1,575	3,959	52.99
		70	1,161	3,680	55.81
		80	1,156	3,693	57.28
		90	1,097	3,674	57.08
		100	955.2	3,533	57.28
	3	110	962.1	3,437	59.82
		50	1,848	4,472	35.48
		60	1,249	3,850	42.69
		70	1,241	3,739	44.70
		80	1,044	3,376	44.90
		90	1,052	3,380	48.41
	4	100	1,045	3,376	48.98
		110	1,033	3,506	46.45
		30	2,241	4,661	
		40			37.76
		50	1,561	3,949	46.18
		60	1,320	3,965	47.49
	5	70	1,205	3,672	46.13
		80	1,271	3,668	46.87
		90	1,086	3,896	48.37
		100	977.1	3,462	51.56
		30	2,319	4,937	23.55
		40	1,827	4,613	33.13
	6	50	1,739	4,283	33.87
		60	1,326	3,806	43.07
		70	1,185	3,545	43.31
		80	1,015	3,526	43.49
		90			45.35
		100	1,041	3,728	44.72
	7	40	1,443	4,146	40.33
		50	1,362	3,739	45.99
		60	1,011	3,563	45.69
		70	1,016	3,556	45.20
		80	1,006	3,442	46.46
		90	1,016	3,463	46.88
8	100	835.1	3,238	44.58	
	30	2,442	5,090		
	50	1,743	4,242	40.59	
	60	1,408	3,880	42.09	
	70	1,273	3,721	46.59	
	80	1,161	3,724	43.95	
IBoA Emul (<i>t</i> -BHP)	1	90	1,050	3,700	43.81
		100			41.76
		110	916/2	3,523	42.75
		20	766.8	3,226	32.95
		30	601.6	2,773	
		40	428.9	2,519	40.71
IBoA Emul (<i>t</i> -BHP)	1	50	429.4	2,512	41.21
		60	421.4	2,457	45.13
		70	438.1	2,437	46.80
		80	381.0	2,298	47.81
		90	340.8	2,225	47.15
		100	340.8	2,225	47.15
IBoA Emul (<i>t</i> -BHP)	1	50	479.5	3,293	152.6
		60	314.6	2,624	163.2
		70	531.7	3,220	167.8
		80	405.3	2,838	172.1
		90	455.4	2,779	180.6

TABLE VIII *Continued*

Recipe type	Run no.	Sample time (min)	M_n (10^{-3} g/mol)	M_w (10^{-3} g/mol)	Unsw. part. radius (nm)
		100	447.3	2,914	187.4
		110	507.5	2,907	192.0
		120	602.5	3,082	200.8
	2	40	1,497	4,226	144.03
		50	1,298	4,015	150.43
		60	1,281	3,678	156.7
		70	1,322	3,783	163.17
		80	1,185	3,609	158.03
		90	1,187	3,631	164.96
		100	1,111	3,517	166.45
		110	1,124	3,585	160.94
	3	70	1,438	4,038	67.58
		80	1,071	3,286	69.58
		90	1,019	3,313	70.72
		100	930.7	3,146	68.42
		110	924.3	3,468	71.54
		120	958.2	3,446	71.36
	4	70	921.5	3,431	50.88
		80	856.7	3,495	52.78
		90	991.1	3,685	55.95
		100	810.0	3,574	56.78
		110	820.5	3,517	52.31
		120	775.9	3,433	53.93
	5	40	921.6	3,357	57.23
		50	1,084	3,396	56.95
		60	845.1	3,231	58.45
		70	878.7	3,231	60.01
		80	788.5	3,121	59.88
		90	823.1	3,107	60.50
		100	733.2	2,834	61.36
		110			60.56
	6	50	204.6	2,386	41.39
		60	163.1	2,263	49.06
		70	227.6	2,502	49.25
		80	252.9	2,538	49.68
		90	233.6	2,524	50.12
		100	245.0	2,520	52.86
		120	277.7	2,553	51.53
	7	40	1,070	3,755	41.67
		50	993.9	3,576	48.85
		60	833.9	3,387	47.49
		70	909.1	3,556	47.75
		80	776.0	3,389	
		90	779.1	3,488	48.39
		100			47.67
		110	781.4	3,422	51.99
	8	40	894.9	3,349	40.62
		50	874.1	3,281	43.94
		60	813.2	3,457	43.22
		70			45.29
		80	837.0	3,528	47.11
		90	723.7	3,213	46.12
		100			46.03
		110	792.5	3,466	47.14
		120	652.7	3,340	
	9	30	804.2	3,610	43.67
		40	724.3	3,504	46.11
		50	789.6	3,493	47.99
		60	752.3	3,612	46.66
		70	887.2	3,485	46.12
		80	869.3	3,525	46.99
		90	930.2	3,540	45.28
	10	10	441.0	3,169	43.99
		20	562.1	3,686	52.45
		30	498.9	3,276	49.61

TABLE VIII *Continued*

Recipe type	Run no.	Sample time (min)	M_n (10^{-3} g/mol)	M_w (10^{-3} g/mol)	Unsw. part. radius (nm)
IBoA ME (KPS)	1	40	419.7	3,227	49.59
		50	414.9	3,150	48.17
		60			47.34
		70			50.76
		80	455.8	3,289	51.02
		110	480.3	3,281	
		40	2,199	4,519	97.73
		60	1,673	4,054	100.8
		70	1,497	3,797	97.85
		80	1,460	4,079	101.1
		90	1,216	3,679	102.2
	100	1,141	3,663	102.6	
	2	40	265.2	3,080	94.21
	50	370.6	3,189	93.70	
	60	321.0	3,053	97.19	
	70	342.3	3,103	95.55	
	80	353.9	3,001	98.66	
	100	281.8	2,946	99.73	
	120	295.1	2,745	100.26	
	3	30	2,451	4,673	90.09
	40	1,884	4,379	88.40	
	50	1,497	3,714	93.66	
	60	1,165	3,688	92.53	
	80	1,150	3,474	96.14	
	90	1,186	3,795	99.41	
	100	1,059	3,575	96.04	
	4	30	366.4	2,984	91.65
	40	415.2	3,089	90.15	
	50	351.9	2,846	90.99	
	60	372.1	2,946	96.94	
	70	383.1	2,900	94.36	
	80	411.2	2,878	95.38	
	90	432.1	2,894	94.33	
	120	476.9	2,795	96.29	
	5	30	2,141	4,544	77.18
	40	1,867	4,372	82.18	
50	1,330	4,123	87.66		
60	1,241	3,731	90.90		
70	1,081	3,569	93.81		
80	1,021	3,441	90.67		
6	30	735.3	3,084	95.13	
40	634	3,000	88.02		
50	432.2	2,610	90.24		
60	441.3	2,641	89.60		
70	442.1	2,614	91.64		
80	427.0	2,594	88.80		
110	340.0	2,342	90.05		
7	30	2,596	4,608	79.67	
40	1,732	4,150	85.76		
50	1,596	4,055			
60	1,582	3,926	85.83		
80	1,181	3,605	89.10		
90	1,121	3,558	87.53		
100	1,002	3,472	90.01		
8	40	1,120	3,759	79.64	
50	967.4	3,602	77.51		
60	1,010	3,539	77.35		
70	791.8	3,308	77.13		
80	807.0	3,293	79.81		
90	645.6	3,166	80.26		
100	676.0	3,036	80.21		
9	40	1,362	3,674	72.77	
50	981.4	3,399	72.83		
60	900.7	3,221			
70	1,005	3,265	77.05		

TABLE VIII *Continued*

Recipe type	Run no.	Sample time (min)	M_n (10^{-3} g/mol)	M_w (10^{-3} g/mol)	Unsw. part. radius (nm)	
IBoA ME (<i>t</i> -BHP)	1	90	743.5	2,912	76.29	
		100	727.1	2,955	77.25	
		110	689.0	2,948	75.19	
		20	609.1	3,512	106.6	
		30	545.1	3,295	110.4	
		40	546.0	3,254	112.2	
		60	491.8	3,371	106.1	
		90	516.5	3,321	112.3	
		100	431.0	3,202	105.6	
		120	524.5	3,474	102.5	
		2	20	675.2	3,573	104.5
			30	522.1	3,409	100.9
	40		644.0	3,577	102.6	
	60				102.2	
	80		585.6	3,497	100.8	
	100		672.2	3,615	100.0	
	3	120	685.5	3,616	100.6	
		20	532.0	3,273	100.8	
		30	470.6	2,932	100.3	
		40	363.0	3,142	100.7	
		50	404.5	2,966	99.49	
		60	395.2	3,199	99.05	
	4	90	473.0	3,111	97.15	
		20	705.0	3,845	98.33	
		30	752.8	3,898	96.16	
		40	699.9	3,141	95.15	
		50	639.3	3,412	95.90	
		60	586.8	3,271	93.30	
	5	70	476.0	2,817		
		90			96.22	
		100	612.5	2,983		
		110			95.78	
		120			95.70	
		30	1,073	3,923	95.39	
		40	558.6	3,203	92.39	
		50	635.3	3,211	94.42	
		60	636.6	3,294	93.73	
		70	494.5	2,924	91.73	
		80	511.2	2,930	90.78	
		100	424.1	2,648	92.05	
	6	30	926.4	3,767	87.67	
		40	778.5	3,125	90.96	
		50	593.7	3,028	94.44	
		60	655.8	3,115	93.47	
		70	534.9	2,869	92.23	
		80			93.31	
	7	90	596.9	2,926	91.83	
		110	396.7	2,703	92.46	
30		363.1	3,161	82.45		
40		277.8	2,695	80.41		
50		278.9	3,006	83.35		
60		249.1	3,877	81.66		
8	70	260.9	2,686	85.31		
	90	234.4	2,808	83.43		
	120	305.4	2,835	85.10		
	20	976.1	4,034	88.07		
	30	793.1	3,425	87.81		
	40	547.3	3,091	82.54		
	50	469.6	2,969	87.95		
	60	504.6	3,133	87.80		
	70			85.47		
	80	542.4	3,061	86.35		
	110	449.3	3,015	86.48		

ones. Under normal circumstances, these small droplets will rapidly disappear by Ostwald ripening. However, given the low water-solubility of the monomer, and the presence of hydrophobic oligomers, these daughter droplets may survive long enough to initiate polymerization. At that point, the polymer within the new particles will be sufficient to protect them against Ostwald ripening, and additional surfactant from the aqueous phase will adsorb onto their surfaces, providing stability against coalescence. With either explanation of nucleation, it may be necessary to invoke monomer exchange via collision, since monomer transport via diffusion may be inadequate as described earlier. This mechanism is similar to the one proposed by Zerfa and Brooks for transfer of radicals from one droplet to another due to collision in suspension reactions.¹³

For the miniemulsions, the issue is not one of forming the small droplets, since the combined use of surfactant and sonication brings about that result quite effectively. Oligomers formed in the aqueous phase will absorb into the miniemulsion droplets causing droplet nucleation.

Molecular weights

Molecular weights and other data are shown in Table VIII. Molecular weights showed no particular trends with respect to polymerization type (emulsion versus miniemulsion) or initiation system (KPS thermal versus *t*-BHP redox). Polydispersities were approximately 4, indicating a significant level of branching, as would be expected in the higher molecular weight acrylates.

SUMMARY

The results of dispersed-phase polymerization of IBoA can be summarized as follows:

- The particle nucleation phenomena in emulsion and miniemulsion polymerization follow the general trends described by Vanderhoff.⁵ For emulsion polymerization, as the surfactant concentration is increased, there is a transition from homogenous to micellar nucleation near the CMC, then a drop in nucleation rate at high surfactant concentration due to insufficient radical flux to support more nucleation. For miniemulsion polymerization, a slow rate of growth of (droplet) nucleation with surfactant concentration is seen, followed (at the CMC) by an increase in the rate of nucleation with added surfactant as the mode of nucleation switches to micellar.
- There is a delay in the conversion time curves caused by slow nucleation. This is due to slow

growth of oligomers generated from the water-soluble initiator, and possible to trace amounts of inhibitor as discussed by Schork and Back.¹⁰

- Emulsion polymerization with both initiators show a strong sensitivity of the particle number and polymerization rate to surfactant level. The effect is less pronounced in high surfactant KPS systems, because of the surface active nature of the ionic chain ends derived from the KPS.
- Miniemulsion polymerizations with both initiators show a relative insensitivity of the particle number and polymerization rate to surfactant level. This is due to the nature of droplet formation in miniemulsions.
- IBoA is sufficiently insoluble in the aqueous phase that emulsion polymerization may or may not be reaction-limited as is always assumed for the emulsion polymerization of more water-soluble monomers.

NOMENCLATURE

A_{drop}	Surface area of droplets per unit volume of aqueous phase, (m^2/L)
d_p	Polymer density (g/m^3)
D_w	Diffusivity of monomer in the aqueous phase (m^2/s)
g	Acceleration due to gravity (m/s^2)
K	a Mark-Houwink-Sakurada parameters for polymer/solvent pair
k_c	Mass transfer coefficient (m/s)
k_p	Propagation rate constant ($\text{L}/\text{mol s}$)
m_M	Mass monomer in recipe (g)
$[M]_p$	Monomer concentration within particles (mol/L)
\bar{n}	Mean active radicals per particle
N_A	Avogadro's number (mol^{-1})
N_p	Particle concentration (mol/L or $\text{no.}/\text{L}$)
Q_M	Maximum mass transfer rate from droplets ($\text{mol}/\text{L s}$)
\bar{r}	Mean (unswollen) (number average) radius of particles (nm)
R_p	Polymerization rate ($\text{mol}/\text{L s}$)
V_s	Swollen particle volume (L)
v_{sett}	Settling velocity (m/s)
V_W	Aqueous phase volume (L)
x	Fractional conversion (mass basis)
$\Delta\rho$	Density difference, particles versus aqueous phase (g/m^3)
$[\eta]$	Polymer intrinsic viscosity (mL/g)
μ	Aqueous phase viscosity ($\text{kg}/\text{m s}$)

References

1. Brandrup, J.; Immergut, E.; Grulke, E.; Akihiro, A.; Bloch, D. Eds. *Polymer Handbook*, 4th ed.; Wiley: New York, 1999.

2. Rodriguez, F. Principles of Polymer Systems, 4th ed.; Hemisphere Publishing: New York, 1989.
3. Ghielmi, A.; Storti, G.; Morbidelli, M. Chem Eng Sci 2001, 56, 937.
4. Skelland, A. H. P. Diffusional Mass Transfer; Krieger: Malabar, FL, 1985.
5. Vanderhoff, J. W. Chem Eng Sci 1993, 48, 210.
6. Hamersveld, E. M. S. V. M. S. Dissertation, Technische Universiteit Eindhoven, The Netherlands, 1999; pp 48–49.
7. Perry, R. H., Ed. Perry's Chemical Engineers' Handbook, 6th ed.; McGraw-Hill: New York, 1984.
8. Vanderhoff, J. W. J Polym Sci Polym Symp 1985, 72, 168.
9. Chai, X.-S.; Schork, F. J.; DeCinque, A.; Wilson, K. Ind Eng Chem Res 2005, 44, 5256.
10. Schork, F. J.; Back, A. J. J Appl Polym Sci 2004, 94, 2555.
11. Reimers, J. L.; Skelland, A. H. P.; Schork, F. J. Polym React Eng 1995, 3, 235.
12. Wang, S.-T.; Poehlein, G. W. J Appl Polym Sci 1994, 51, 597.
13. Zerfa, M.; Brooks, B. W. Chem Eng Sci 1997, 52, 2423.